Optimisation of Lambertian Order for Indoor Non-directed Optical Wireless Communication

D. Wu, Z. Ghassemlooy, H. Le Minh and S. Rajbhandari
Optical Communications Research Group, School of Computing, Engineering and Information Sciences
Northumbria University, Newcastle Upon Tyne, UK
E-mail: {dehao.wu; z.ghassemlooy}@northumbria.ac.uk

M.A.Khalighi
Ecole Centrale Marseille, Institute Fresnel
Marseille, France
E-mail: Ali.Khalighi@Fresnel.fr

X. Tang
Optical Communications Research Group, School of Computing, Engineering and Information Sciences
Northumbria University, Newcastle Upon Tyne, UK

***Abstract*— This paper studies the optimised Lambertian order (OLO) of light-emitting diodes (LEDs) for an indoor non-directed line of sight optical wireless communication (NLOS-OWC) systems. We firstly derive an expression of the OLO from a conventional Lambertian LED model, Then, we analyse the indoor multi-cell NLOS-OWC channel characteristics including optical power distribution and multipath time dispersion for two cases of one-cell and four-cell configurations. Furthermore, we estimate the transmission bandwidth by simulating the channel frequency response. Numerical results show that, by using OLO a significant improvement of the transmission bandwidth can be achieved for in indoor NLOS-OWC systems, in particular, for multi-cell configurations.**

Keywords- Optimum Lambertian order, LED, optical wireless communication and root mean square (RMS) delay spread.

I. INTRODUCTION

LEDS are being widely used as sources in short-range indoor optical wireless communication (OWC) links for local area network (LAN) [1, 2]. They promise numerous advantages compared with the conventional radio frequency (RF) systems, such as offering a potential huge bandwidth, a secure links as rays cannot penetrate walls or opaque objects, and freedom from spectrum regulation and licensing. Due to the fast dynamic response of most current available LEDs, they can be modulated with fast switches, enabling high transmission data rates. With the increasing popularity of high definition television and video over the internet, the indoor OWC access technology employing LEDs becomes one possible and economical solution to address the bandwidth congestion currently being experiencing in most access networks [3, 4].

The NLOS-OWC links with intensity modulation and direct detection is a suitable candidate for high speed indoor communication systems [5, 6]. Compared with line-of-sight (LOS) transmission, NLOS links offer a larger coverage area and an excellent mobility and without any need to precise alignment or a tracking mechanism. On the other hand, compared with the common diffuse configurations [7], NLOS-OWC links provide a lower path loss, lower intersymbol interference (ISI) caused by multipath reflections, and a higher transmission bandwidth. Therefore, NLOS-OWC links employing wide-angle transmitters and receivers are more convenient to use, particularly for mobile terminals.

Most current research on NLOS-OWC systems focuses on uniform received power distribution as well as on the techniques to decrease the ISI. A uniform received power distribution for NLOS-OWC systems using a novel genetic algorithm is proposed in [8, 9] without increasing the multipath distortion. In [10], the authors introduced a novel LED arrangement to reduce SNR fluctuations. Analysis of multipath time dispersion of the indoor OWC channel has been made for NLOS-OWC systems in [11, 12]. It is shown that less multipath distortion can be achieved by optimising the divergence angle of the LED and by employing some special configuration. A more uniform power distribution is proposed in [13, 14] and a reduced ISI is achieved by using a holographic diffuser. Spotlight is implemented for the high data rate transmission in [15], and the results show that indoor NLOS-OWC links employing LEDs with small divergence angles have less channel distortion than those with large divergence angles. Therefore, to achieve a higher transmission bandwidth and a more uniform power distribution, multi-cell NLOS-OWC systems are the preferred solution. However, previous studies have not analysed the Lambertian order and its impact on the time dispersion and channel transmission bandwidth. As a matter of fact, the divergence angle is an essential parameter of a LED and it significantly affects the received power distribution and the channel distortion in indoor NLOS-OWC systems.

In this paper, a multi-cell NLOS-OWC links with OLO is proposed. Using the conventional Lambertian model, we derive a new expression for the OLO. Then, we investigate the received power distribution for two cases of one-cell and four-cell configurations, considering optimised and nonoptimised LED divergence angles. To estimate the multipath time dispersion of the channel, the root-mean-square (RMS) delay spread with and without angle optimization are simulated. Lastly, the transmission bandwidth of the proposed multi-cell NLOS-OWC channel is analysed.

The rest of the paper is organized as follows. In Section II, we present the system configuration, and describe the channel DC gain, OLO, and multipath characteristics. In Section III, we present some numerical results to study the channel characteristics in different scenarios of LED positioning and angle distribution. Finally, the conclusions of this work are summarized in Section IV.

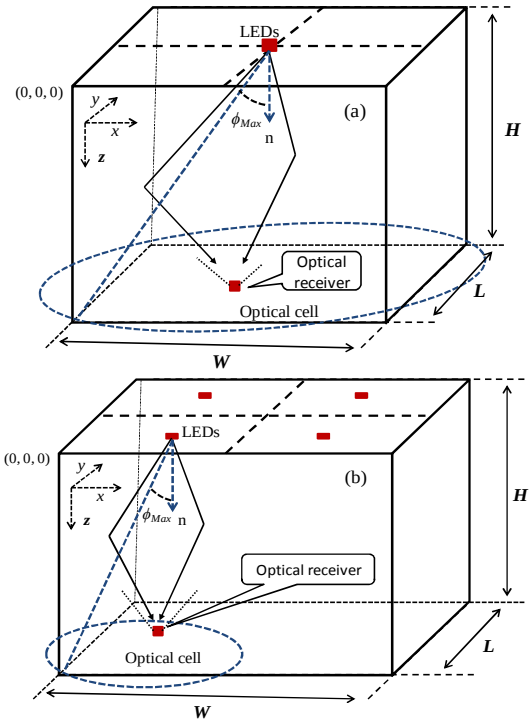

Fig. 1. Indoor non-directed cellular OWC: systems a) one cell and b) four cells.

II. System Description

A. System configuration

The proposed one-cell and four-cell indoor NLOS-OWC systems are shown in Fig.1. The link depicted in Fig.1(a) has only one cell to cover the receiver plane, which employs a group of LEDs with large divergence angles. The footprint of this one-cell system has its value at the cell center and its minimum at the cell edge. To achieve a more uniform power distribution, a four-cell topology can be applied as shown in Fig.1(b). Each cell has a group of LEDs mounted at the cell center with specified divergence angles. At the receiving end, the optical receiver, mounted on a mobile terminal, has a dedicated FOV to ensure seamless connectivity.

B. Channel model with Lambertian source

The emission from a LED can be modeled using a generalized Lambertian radiant intensity [16]. In NLOS-OWC configurations, the transmitters, located at the ceiling, point downward to the floor and the receiver is pointed to the ceiling. The DC gain of the indoor LOS OWC channel is given by [16]:

$$H(0) = \begin{cases} \dfrac{(m+1)A}{2\pi d^2}\cos^m(\phi)T_s(\theta)g(\theta)\cos(\theta), & 0 \le \theta \le \varphi_c, \\ 0, & \theta \ge \varphi_c \end{cases} \tag{1}$$

where A is the photodetector surface area, ϕ is the irradiance angle, θ is incidence angle, φ_c is the FOV (semiangle) of the receiver and d is the distance between transmitter and receiver. $T_S(\theta)$ is the optical filter gain, and $g(\theta)$ is the optical concentrator gain. m is the Lambertian radiant order relating to the transmitter semiangle $\varphi_{1/2}$, (at half power), which is given by [16]:

$$m = -\frac{\ln 2}{\ln(\cos\varphi_{1/2})}, \tag{2}$$

The received optical power of the LOS path is given by:

$$P_{\text{Rx LOS}} = P_{\text{Tx}}\, H(0). \tag{3}$$

where, P_{Tx} is the overall transmitted optical power of LEDs.

C. Optimum Lambertian order

In indoor NLOS-OWC systems, the received optical power consists of the power from the LOS path and the reflected paths. Due to the different propagation delays of different paths, the multipath ISI would limit the transmission bandwidth. To circumvent this problem and to achieve a high transmission bandwidth, the optical power from the LOS path should be maximized, and also, the multipath ISI caused by reflection should be minimised. The received optical power fromthe LOS can be calculated using (1) to (3). For each cell shown in Fig.1, the received optical power is maximum at $\phi = 0$ and minimum at $\phi = \phi_{\text{Max}}$. The corresponding minimum received power is given by (1) and (3):

$$P_{\text{Min}} = P_{\text{Tx}}\frac{(m+1)A}{2\pi {d_{\text{Max}}}^2}\cos^m(\phi_{\text{Max}})T_s(\theta)g(\theta)\cos(\theta), \quad 0 \le \theta \le \varphi_c, \tag{4}$$

where d_{Max} is the maximum distance between the transmitter and the receiver within a cell, and ϕ_{Max} is the corresponding maximum irradiance angle. The partial derivation (4) in terms of the Lambertian order m is given by:

$$\frac{\partial P_{\text{Min}}}{\partial m} = P_{\text{Tx}}\,T_s(\theta)g(\theta)\cos(\theta)\frac{A}{2\pi {d_{\text{Max}}}^2}\cos^m(\phi_{\text{Max}}) \times \{1 + (m+1)\ln(\cos(\phi_{\text{Max}}))\}, \tag{5}$$

where, parameter $K = P_{\text{Tx}}\,T_s(\theta)g(\theta)\cos(\theta)\frac{A}{2\pi {d_{\text{Max}}}^2}$ is independent of m. Therefore, (5) can be simplified to:

$$\frac{\partial P_{\text{Min}}}{\partial m} = K\cos^m(\phi_{\text{Max}})\{1 + (m+1)\ln(\cos(\phi_{\text{Max}}))\}, \tag{6}$$

To find the OLO m_{opt}, we set $\frac{\partial P_{\text{Min}}}{\partial m} = 0$, m_{opt} is given by (2):

$$m_{\text{opt}} = \frac{-1}{\ln(\cos(\phi_{\text{Max}}))} - 1, \tag{7}$$

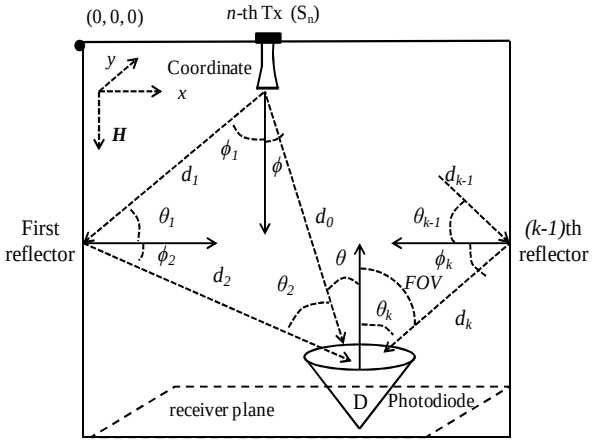

Fig.2. Geometry of source, detector and reflector

From (2) and (7), we can calculate the optimum transmitter semiangle $\varphi_{1/2\,\mathrm{opt}}$ at half power, which is:

$$\varphi_{1/2\,\mathrm{opt}} = \cos^{-1}\left(\exp\left(\frac{-\ln(2)}{\frac{-1}{\ln(\cos(\phi_{\mathrm{Max}}))}-1}\right)\right), \quad 0 < \varphi_{1/2\,\mathrm{opt}} < 90^{o}. \tag{8}$$

D. Multipath characteristics

In high data rate indoor NLOS-OWC systems, the path loss and the multipath-induced time dispersion limit the link performance. The maximum available data rate can be predicted if the channel impulse response $h(t)$ and the RMS delay spread are known. As the configurations shown in Fig.2, the optical power distribution and the multipath dispersion at the receiver plane can be characterized by the channel impulse response $h(t)$. For a NLOS-OWC channel, using (1) and (2), the impulse response for a particular source S and a detector D (x, y, z), is given by [11]:

$$h^{0}(t;S,D) = \frac{(m+1)A}{2\pi d^{2}}\cos^{m}(\phi)T_{s}(\theta)g(\theta)\cos(\theta)\mathrm{rect}(\frac{\theta}{\varphi_{c}})\delta(t-\frac{d_{0}}{c}), \tag{9}$$

where d is the LOS distance between S and D and c is the speed of light. The rectangular function $\mathrm{rect}(x)$ is given by:

$$\mathrm{rect}(x) = \begin{cases} 1 & \text{for } |x| \le 1, \\ 0 & \text{for } |x| > 1. \end{cases} \tag{10}$$

Assuming that all reflectors (i.e. plaster and acoustic-tiled walls, unvarnished wood) are approximately Lambertian [16], the channel impulse response with multiple optical sources and multiple reflections is [17]:

$$h(t;\,S,D) = \sum_{n=1}^{N_{source}}\sum_{k=0}^{\infty} h_{n}^{k}(t;\,S,D) \tag{11}$$

The channel impulse response for k-bounce is given by [18]:

$$h^{k}(t;\,S,D) = \int_{\Psi}\left[\xi_{0}\xi_{1}\ldots\xi_{k}\rho^{k}\,\mathrm{rect}(\frac{\theta_{k}}{\varphi_{c}})\times\,\delta(t-(\frac{\sum_{k=0}^{\infty}d_{k}}{c}))\right]dA_{ref}\ ,\ k\ \ge 1 \tag{12}$$

where

$$\xi_{0} = \frac{(m+1)A}{2\pi d^{2}}\cos^{m}(\emptyset_{1})\cos(\theta_{1})\,dA_{ref}\cos\theta_{1}$$

$$\xi_{1} = \frac{dA_{ref}\cos\emptyset_{2}\cos\theta_{2}}{\pi d_{2}^{2}}$$

, … ,

$$\xi_{k} = \frac{A\,\cos\emptyset_{k+1}\cos\theta_{k+1}}{\pi d_{k+1}^{2}}T_{s}(\theta_{k+1})g(\theta_{k+1}).$$

The integration in (12) is performed with respect to the surface Ψ of all reflectors, dA_{ref} is the small area of the reflecting element, ϕ_k and θ_k are the angles of irradiance and incidence, respectively, and d_k is the distance from k bounces to the detector (see Fig. 2).

The RMS delay spread is given by [19]:

$$S = \left[\frac{\int(t-\mu)^{2}h^{2}(t)dt}{\int h^{2}(t)dt}\right]^{\frac{1}{2}} \tag{14}$$

where μ is the mean delay given by:

$$\mu = \frac{\int t\,h^{2}(t)dt}{\int h^{2}(t)dt} \tag{15}$$

where t is the delay time of propagation.

III. Numerical Results and Discussion

Here, we present some numerical results to study the channel characteristics of multi-cell indoor NLOS-OWC systems. The specifications and parameters are given in Table I. Two different configurations are considered and simulated.

A. Optical power distribution

The spatial distributions of the received power from LOS for the one-cell and four-cell configurations are shown in Fig. 3(a) to (d) for the cases of nonoptimised and optimised divergence angles. From Fig. 3(a), we notice that for the case of one-cell configuration with a typical (nonoptimised) FWHM (Full width at half maximum) divergence angle of 120^{o}, the received power varies between -5.8 dBm to -13.3 dBm. Using (8), the optimised FWHM angle of LED is ~108^{o} and the corresponding OLO is ~1.3. The received power for the OLO case varies between -5.2 dBm to -13.3 dBm as can be seen in Fig. 3(b). Comparing Figs. 3(a) and (b), we notice that the maximum received power from LOS is only slightly increased by optimising the divergence angle.

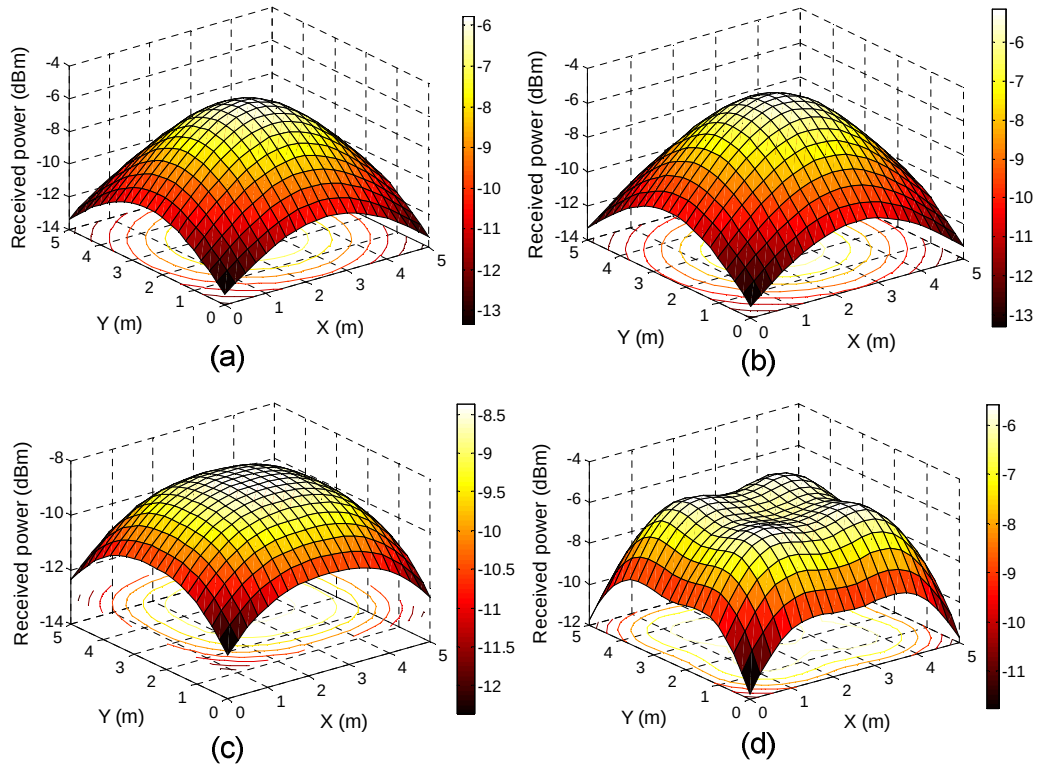

Fig. 3. Spatial distribution of the received power: (a) One-cell with 120° FWHM angle , (b) One-cell with the optimum 108° FWHM angle, (c) Four-cell with 120° FWHM angle and (d) Four-cell with the optimum 56° FWHM angle.

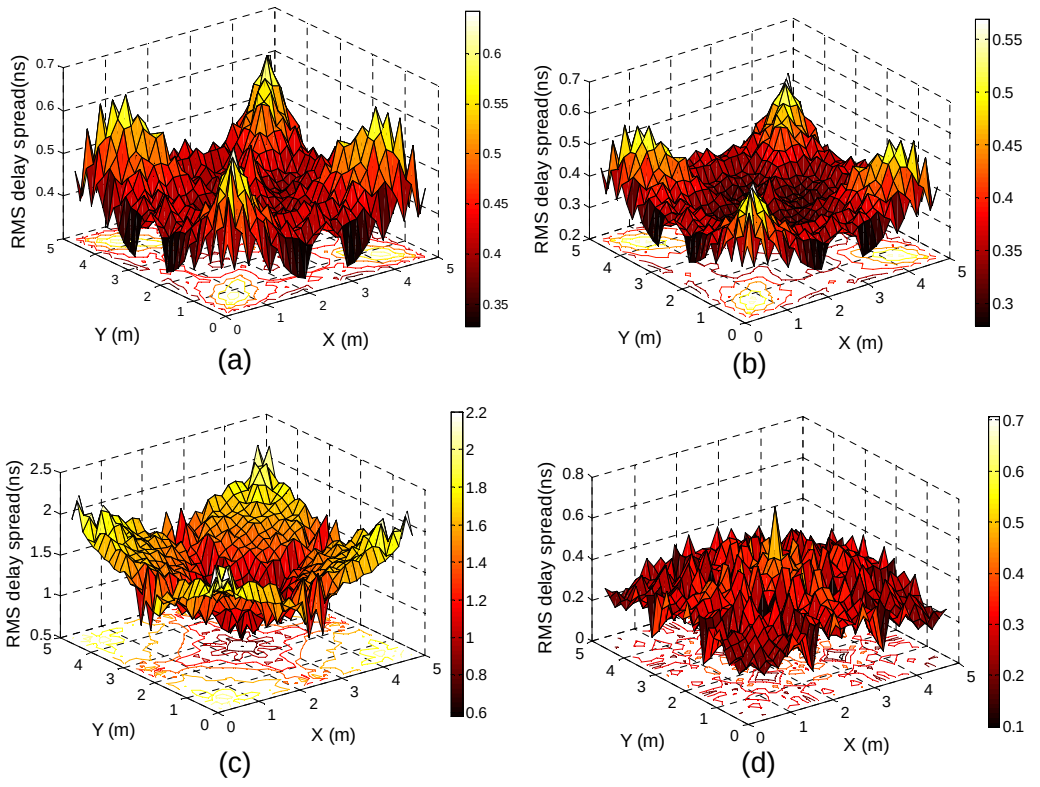

Fig. 4. Spatial distribution of RMS delay spread: (a) One-cell with 120° FWHM angle , (b) One-cell with 108° FWHM angle, (c) Four-cell with 120° FWHM angle and (d) Four-cell with 56° FWHM angle.

TABLE I
SPECIFICATION FOR INDOOR NLOS OWC SYSTEMS

LED wavelength (λ)	(500~1000) nm
LED launched power	200 mW
LED interval	0.05 m
Room (length, width, height)	$5 \times 5 \times 3$ m^3
Half angle FOV of receiver	60 (deg)
Surface area of photodiode	1 cm^2
Gain of an optical filter	1.0
Refractive index of a lens at a photodiode	1.5
Reflection coefficient (wall, ceiling, floor)	(0.8, 0.8, 0.3)
One-cell configuration	
Number of LEDs per cell	144
Four-cell configuration	
Number of LEDs per cell	36
Cell size	2.5×2.5 m^2

Similarly, Fig. 3(c) and (d) compare the received power of four-cell configuration with and without divergence angle optimization, respectively. From (8), the optimised FWHM angle of LED is 56^o and corresponding OLO is ~5.57. The received power varies between -8.4 dBm and -12.4 dBm for nonoptimised angle (120^o FWHM) and between -5.6 dBm and -11.7 dBm for optimised angle. In this case, angle optimization allows 0.7 dB and 2.8 dB increase for minimum and maximum received powers, respectively.

B. *RMS delay spread*

As the receiver performance could considerably be affected by ISI, we investigate the channel time dispersion for the proposed configurations, Fig.4 (a) to (d) show the RMS delay spreads of different configurations with and without angle optimization. We notice that the optimised and nonoptimised secenarios have similar distributions and the RMS delay spread varies 0.3 ns and 0.6 ns for the one-cell systems. The maximum RMS delay spread occurs at the positions (0.5, 0.5, 3) m, (0.5, 4.5, 3) m, (4.5, 0.5, 3) m and (4.5, 4.5, 3) m.

For the four-cell configuration, we see from Fig. 4(c) and (d) that the maximum RMS delay spreads correspond to the positions (0, 0, 3) m, (0, 5, 3) m, (5, 0, 3) m and (5, 5, 3) m for the nonoptimised case, and (2, 2, 3) m, (4, 2, 3) m, (2, 4, 3) m and (4, 4, 3) m for the optimised case. There is a significant RMS reduction after optimization: it decreases from 1.5 ns to 0.4 ns.

C. *Transmission bandwidth*

Since the largest multipath distortion occurs at the point with maximum RMS delay spread in a room, the transmission bandwidth constraint can be estimated by simulating the frequency response at this point. Following the above analyses of maximum RMS delay spread for different configurations, the normalized channel frequency responses at the position corresponding to the largest RMS delay spread point for the one-cell and four-cell systems are plotted in Fig. 5. We notice that the -3 dB transmission bandwidth of the optimised one-cell system is ~94 MHz, which is slightly larger than the 91 MHz bandwidth of the nonoptimised case. For the case of four-cell system, the -3 dB transmission bandwidth for the optimised four-cell configuration has a significant improvement compared to the nonoptimised one: it increases form 39 MHz for nonoptimised configuration to 185 MHz with angle optimization.

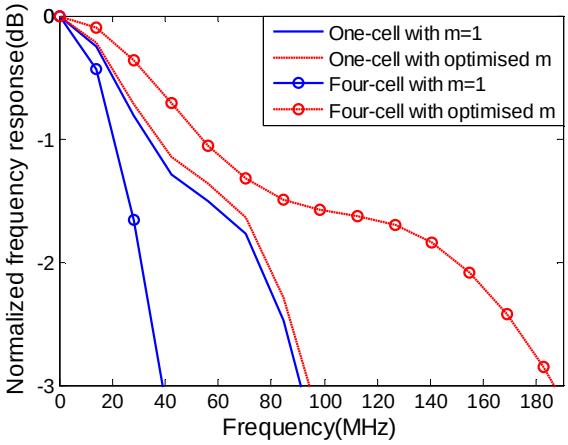

Fig. 5. The channel frequency response at maximum RMS delay spread point for one-cell and four-cell configurations

IV. CONCLUSION

In this paper, we derive the OLO for a particular room configuration and analyse the performance of one-cell and four-cell systems using optimum and nonoptimum Lambertian orders. The channel characteristics including optical received power distribution and multipath dispersion are simulated and analysed. The results show that the received optical power and the transmission bandwidth can be improved with optimisation. While this improvement factor depends on the room dimension and the number of cells, it is much more significant for multi-cell configurations.

ACKNOWLEDGMENT

The authors would like to acknowledge the support by EU FP7 Cost Actions of 1101.

REFERENCES

[1] H. Elgala, R. Mesleh, and H. Haas, "Indoor optical wireless communication: potential and state-of-the-art," *Communications Magazine, IEEE*, vol. 49, pp. 56-62, 2011.

[2] L. Xia, J. Vucic, V. Jungnickel, and J. Armstrong, "On the Capacity of Intensity-Modulated Direct-Detection Systems and the Information Rate of ACO-OFDM for Indoor Optical Wireless Applications," *Communications, IEEE Transactions on*, vol. 60, pp. 799-809, 2012.

[3] D. O'Brien, G. Parry, and P. Stavrinou, "Optical hotspots speed up wireless communication," *Nature Photonics*, vol. 1, pp. 245-247, 2007.

[4] R. J. Green, H. Joshi, M. D. Higgins, and M. S. Leeson, "Recent developments in indoor optical wireless systems," *IET Communications*, vol. 2, pp. 3-10, 2008.

[5] N. Hayasaka and T. Ito, "Channel modeling of nondirected wireless infrared indoor diffuse link," *Electronics and Communications in Japan*, vol. 90, pp. 9-19, 2007.

[6] J. B. Carruthers and J. M. Kahn, "Modeling of nondirected wireless Infrared channels," *IEEE Transaction on Communication*, vol. 45, pp. 1260-1268, 1997.

[7] Z. Ghassemlooy and A. R. Hayes, "Optical wireless communication systems - Part I: Review," 2003.

[8] D. Jupeng, H. Zhitong, and J. Yuefeng, "Evolutionary Algorithm Based Power Coverage Optimization for Visible Light Communications," *Communications Letters, IEEE*, vol. 16, pp. 439-441, 2012.

[9] M. D. Higgins, R. J. Green, M. S. Leeson, and E. L. Hines, "Multi-user indoor optical wireless communication system channel

control using a genetic algorithm," *Communications, IET*, vol. 5, pp. 937-944, 2011.

[10] W. Zixiong, Y. Changyuan, Z. Wen-De, C. Jian, and C. Wei, "Performance of a novel LED lamp arrangement to reduce SNR fluctuation for multi-user visible light communication systems," *Opt. Express*, vol. 20, 2012.

[11] J. B. Carruthers and S. M. Carroll, "Statistical impulse response models for indoor optical wireless channels," *International Journal of Communication Systems*, vol. 18, pp. 267-284, 2005.

[12] J. B. Carruther and J. M. Kahn, "Angle diversity for nondirected wireless infrared communication," *Communications, IEEE Transactions on*, vol. 48, pp. 960-969, 2000.

[13] D. Wu, Z. Ghassemlooy, M. Hoa Le, S. Rajbhandari, and Y. S. Kavian, "Power distribution and q-factor analysis of diffuse cellular indoor visible light communication systems," in *European Conference on Networks and Optical Communications (NOC)*, Newcastle Upon Tyne UK, 2011.

[14] D. Wu, Z. Ghassemlooy, M. Hoa Le, S. Rajbhandari, and C. Lu, "Channel characteristics analysis of diffuse indoor cellular optical wireless communication systems," *Proc. of SPIE*, vol. 8309, 2011.

[15] T. Borogovac, M. Rahaim, and J. B. Carruthers, "Spotlighting for visible light communications and illumination," in *GLOBECOM Workshops (GC Wkshps), 2010 IEEE*, 2010, pp. 1077-1081.

[16] J. M. Kahn and J. R. Barry, "Wireless infrared communications," *Proceedings of IEEE*, vol. 85, pp. 265-298, 1997.

[17] F. R. Gfeller and U. Bapst, "Wireless in-house data communication via diffuse infrared radiation," *Proceedings of the IEEE*, vol. 67, pp. 1474- 1486, 1979.

[18] L. Kwonhyung, P. Hyuncheol, and J. R. Barry, "Indoor channel characteristics for visible light communications," *IEEE Communications Letters*, vol. 15, pp. 217-219, 2011.

[19] J. B. Carruthers, S. M. Caroll, and P. Kannan, "Propagation modelling for indoor optical wireless communications using fast multi-receiver channel estimation," *IEE Proceedings-Optoelectronics*, vol. 150, pp. 473-481, 2003.